Automated Device to Enable Passive Pronation and Supination Activities of the Hand for Experimental Testing with Cadaveric Specimens: A Collaboration Between The University of New Mexico and New Mexico Institute of Mining and Technology

Jodie Gomez, BS[*†]; Jakub Mroczkowski, BS[‡]; Lauren Long, BS[*]; Christopher A. Buksa, BS[*†]; Deana M. Mercer, MD[*]; Christina Salas, PhD[*†§]; David I. Grow, PhD[*‡]

[*]Department of Orthopaedics & Rehabilitation, The University of New Mexico Health Sciences Center, Albuquerque, New Mexico

[†]Department of Mechanical Engineering, The University of New Mexico, Albuquerque, New Mexico

[‡]Department of Mechanical Engineering, New Mexico Institute of Mining and Technology, Socorro, New Mexico

[§]Center for Biomedical Engineering, The University of New Mexico, Albuquerque, New Mexico

Abstract

In cadaveric research, reproducing physiological conditions under which the specimens would be loaded in vivo is essential to achieve clinical applicability. This is a collaborative study bringing together engineers from The University of New Mexico and New Mexico Institute of Mining and Technology. We describe development of an automated device to enable *passive* pronation and supination of the hand (rotation achieved through direct manipulation) for use in cadaveric experimental testing of the hand, wrist, forearm, or elbow. We present a brief motivation for development of this device, design details, an overview of one possible application, and ways to use this device for *active* pronation and supination activities (rotation achieved through tendon loading). We aim to provide the necessary information for reproduction of this device by other institutions for similar testing purposes.

Introduction

When conducting experimental tests on cadavers, it is essential to reproduce physiological conditions under which the specimens would be loaded in vivo. For example, when performing tests on a femur, it is important to apply a combination of axial, torsional, and bending loads that would normally be applied to the bone while a person walks or runs. These loads can be applied with custom-made testing fixtures that represent the acetabulum and tibial plateau for simulated articulation with the hip and tibia, respectively. Custom fixtures can be attached to a load frame programmed to provide the loading conditions. In the case of the human hand and forearm, the reproduction of physiological motion can be challenging owing to the various bones and soft tissue that allow the hand to move in a variety of ways.

We were tasked with developing an automated system that enabled pronation and supination motions of a cadaveric hand. The device would be used in a study on the contribution of the interosseous membrane and annular ligament to the stability of the radial head.

The goals of the system were as follows: 1) control pronation and supination activities of the hand through an automated mechanism; 2) hold the arm at a 90° elbow-flexion angle while subjecting the forearm to a simulated load through the long axis of the forearm and a load through the biceps brachii tendon attachment on the radius, in line with the muscle pull; 3) enable

high-resolution motion capture of the specimen through strategically placed retroreflective markers; and 4) allow correlation of the motion data at all angles from 45° of pronation to 45° of supination of the hand with the use of frame mounted markers.

Design

We designed a modular and adjustable testing fixture capable of dynamic motion. Multiple pieces immobilized the arm as necessary, controlled specific motions to simulate arm movement, and collected the desired data outputs. These pieces included: a rigid base plate; a linear rail system for adjustability and axial movement; a hand-rotation assembly for guiding pronation and supination activities; a fixation plate for stabilizing the humerus; a pulley system for applied external loads; a high-resolution, motion capture system for determining rotations and translations of specified bones; and a belt-drive system for pronation and supination motions of the hand.

Rigid Base Plate

The rigid base plate consists of a grid of threaded holes that enables adjustments and relocation of the fixture components to accommodate the anatomical variations of each specimen (Figure 1). This allows the fixture to be customized based on the length and width of each specimen. The plate was bolted to a table to ensure rigid and consistent placement of the fixture during testing.

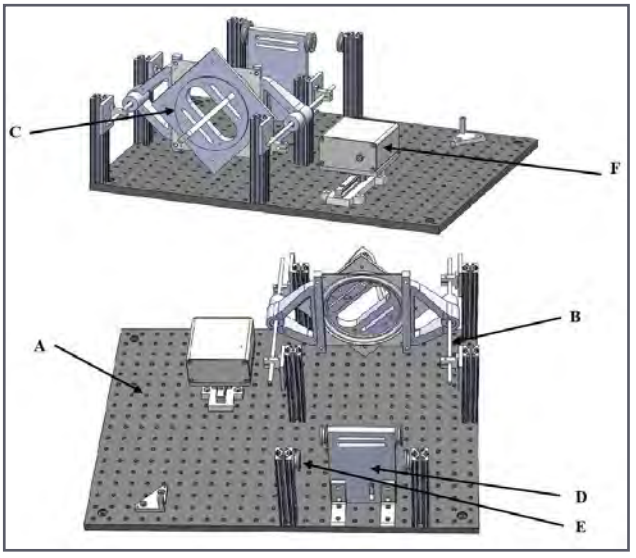

Figure 1. Two oblique views of the full device. Each component is coded by letter and referenced in the body of the article: A, rigid base plate; B, linear rail system; C, hand rotation assembly; D, humerus fixation plate; E, pulley system; and F, motor control system.

Linear Rail System

The linear rail system is fixed to the rigid base plate and hand-rotation assembly. It supports the weight of the hand and forearm, holding them above the base plate (Figures 1, 2A, and 2B). The parallel positioning of the linear rail system enables low-friction movement of the hand-rotation assembly during axial loading (longitudinally).

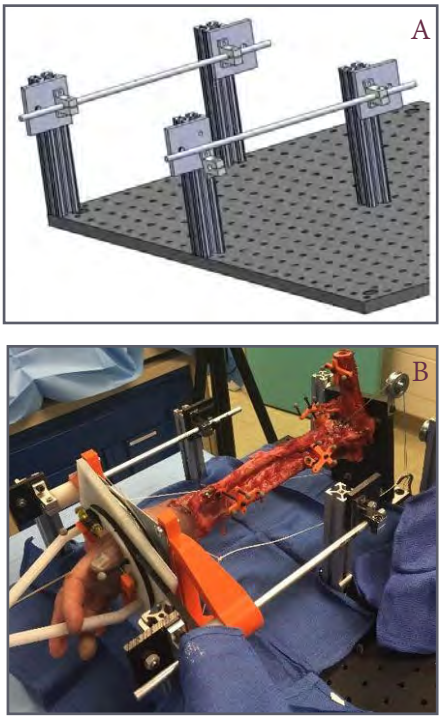

Figure 2. (A) Solid model of linear rail assembly positioned on the base plate. (B) Oblique view of the rail assembly showing parallel positioning on either side of the forearm. These rails allow for suspension of the arm with the hand rotation assembly. Axial compressive forces can be applied to the forearm by loading the hand rotation assembly so that it compresses the forearm toward the humerus fixation plate.

Hand-Rotation Assembly

The hand-rotation assembly consists of multiple parts including a rotation turntable (gray), side extensions (orange), and a front face (white and light blue; Figure 3A). The rotation turntable has a stationary half and a rotating half. The stationary half connects to the linear rails using the extensions on either side of the turntable through bushings. These extensions were computer-modelled and 3D-printed in acrylonitrile butadiene styrene (ABS). This design aligns the long axis of the specimen with the linear rails of the fixture and supports the weight of the specimen. The extensions were fixed to and hold up the stationary half of the turntable.

Between the stationary and rotating halves of the turntable is an array of roller bearings that allow for low-

friction rotation. On the rotating front face, a 3D-printed nylon part supports the hand through a slot and allows fixation of the hand using a K-wire; this part renders rotational motion from the turntable to the hand and forearm (Figure 3B). The design allows for pinning of multiple hand sizes, complete immobilization of wrist flexion, and rotations between full pronation and supination. Extending from the front face of the rotating turntable is a circular shoulder that provides the surface for a rubber belt to be adhered and interfaced with the motor-control system. It also features four locations, where motion capture markers are placed for tracking the angular position of the rotating turntable. The linear rail system and hand-rotation assembly collectively allow for rotation of the forearm and hand about the long-axis of the forearm.

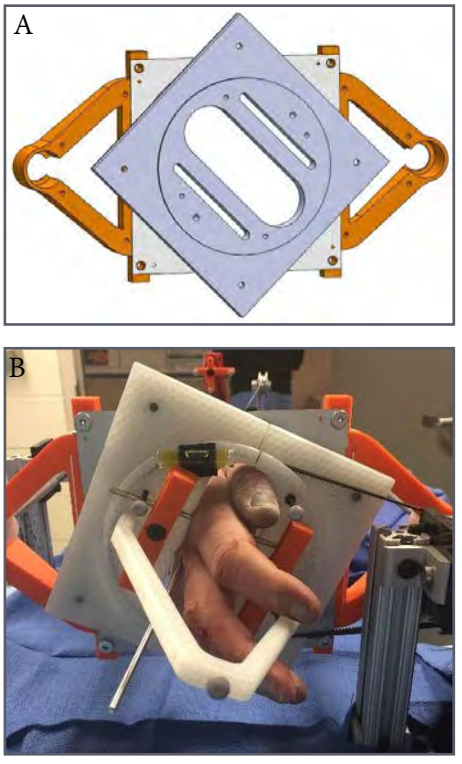

Figure 3. Hand rotation assembly. (A) Solid model. (B) 3D-printed device with hand inserted to describe attachment of the hand to the device.

Humerus Plate

The humerus plate allows for the elbow to be flexed at 90° and raised off the rigid base plate to ensure the motion capture markers move in space without restrictions and remain visible to the motion capture cameras. Option one (Figure 4A): the humerus of the specimen can be bolted to the humerus plate through slots that allow for translation and elevation of the humerus and elbow so that they are aligned with the forearm and hand (within the hand-rotation assembly). The humerus fixture also includes a pulley to route a constant load on the biceps brachii tendon toward the proximal-medial side of the specimen. Notably, there is one pulley mounted on each side of the plate to account for left and right hands. Option two (Figure 4B): the humerus can be attached to the fixation plate through a top mounted piece that surrounds the distal diaphyseal and metaphyseal regions of the bone. This option is fully adjustable, but some pivoting about the top plate can occur if the bone is not seated against the wall of the humerus plate. The pivoting can be corrected by printing a taller top-mounted piece to encapsulate a greater portion of the diapysis.

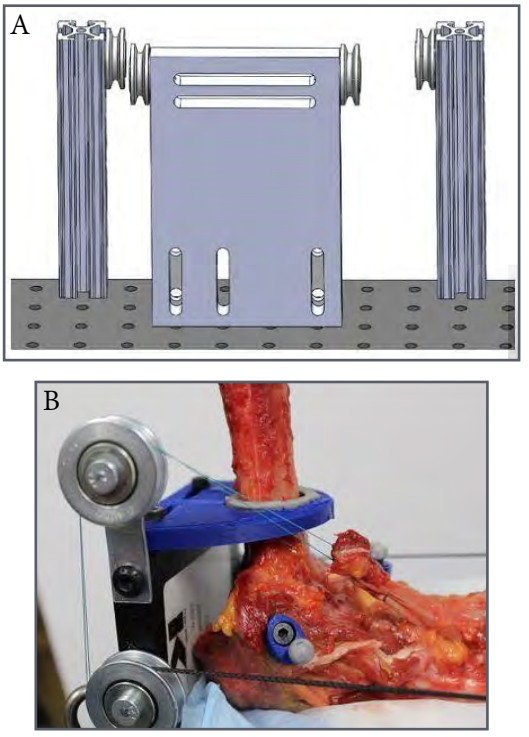

Figure 4. (A) Humerus fixation plate (ie, option one) allowing for fixation of the humerus to the plate through bolts. (B) Option two, allowing for adjustable fixation of the humerus through a top adjustable piece that surrounds the bone.

Pulley System

A series of pulleys are positioned at the back of the fixture, mounted to the rigid base plate (Figure 5). These pulleys divert an axial load applied to the specimen through a Y-weight distributor attached to free-hanging weights. The weights are hung from a cable tied through small holes on either side of the hand-rotation assembly so that the axial load is distributed across the hand-rotation assembly and onto the specimen.

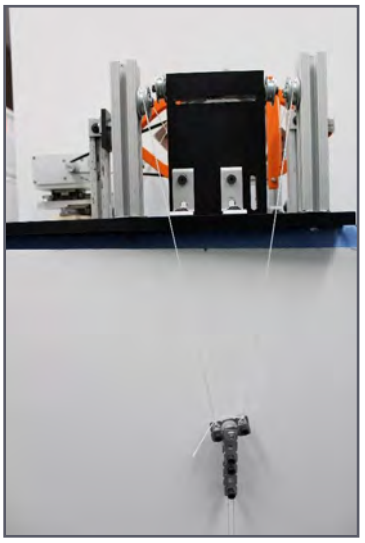

Figure 5. Pulley system showing cables routed through Y-weight distributor for axial loading of the forearm.

Motor-Control System

The motor-control system integrates with the hand-rotation assembly for rotational manipulation of the hand through a full range of pronation and supination angles. Revolution is transmitted through a belt-drive system, where a precision (stepper) motor (NEMA 17, US National Electrical Manufacturers Association, Arlington, Virginia) delivers accurate and repeatable rotations to achieve the targeted position. The device uses an Arduino Uno (Arduino, Ivrea, Italy) programmed to the desired interface through a physical controller.

The main device is housed in a compact assembly positioned on crossed linear rails for belt tightening (x) and for belt alignment with the moving hand-rotation assembly (y; Figure 6A). The device allows for control of the hardware from a distance (3.7-m [12-ft] cable), which enables personnel who are not assisting with the apparatus-end of the study to adjust the position of the forearm. For simplification, the controller includes an analog joystick to control all movement of the device and includes a liquid-crystal display (LCD) screen that displays the status of the forearm's position (Figure 6B). The user can increase or reduce speed of positioning when moving the joystick completely over in one direction (full speed) or only partially over (reduced speed) for a ramped approach. Pushing down on the analog stick returns the motor to its origin or neutral position. Computer code was written that rotates the motor clockwise (while holding the analog right) and counterclockwise (when holding it left). Instead of predesigned increments, the LCD displays the changing angle into both pronation and supination motions in real time and maintains the position until the user stops. The controller plugs into the circuit of the microcontroller and powers both the LCD and analog stick.

Selecting the appropriate motor driver required understanding the device deliverables. Because speed nor force (except enough to exert rotation of the forearm) were critical factors, minimizing the size of the unit was considered along with available precision capabilities. The Mercury SM-4BYG011-25 stepper motor (Mercury Industry, China) with 11.5:1 gear ratio was chosen, effectively allowing 2.645 Nm of torque to be applied to the arm with angular resolution of 0.0049° per step. The control architecture includes an Arduino Uno microcontroller and a DRV8834 stepper motor driver (Pololu Corp, Las Vegas, NV). The selected motor driver allows *microstepping* of up to 1/32-step to allow improved angular resolution of 200 steps per revolution.

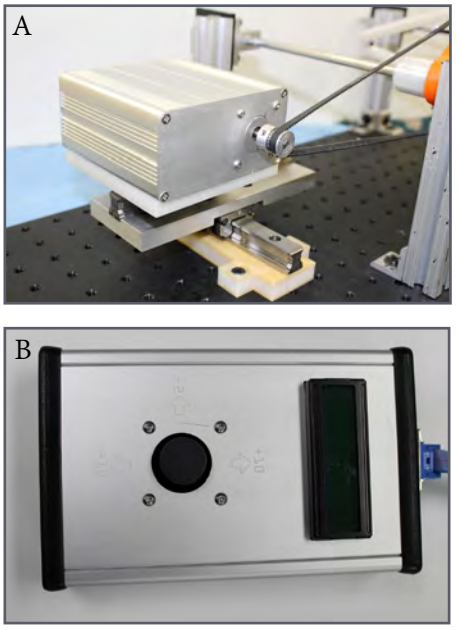

Figure 6. (A) Main motor positioned on crossed linear rails to allow for belt tensioning (x-direction) and alignment with the moveable hand rotation assembly (y-direction). (B) Remote motor controller for positioning of the hand at any angle of pronation or supination. It is connected to the main motor through a 3.7-m (12-ft) cable.

Motion Capture System

The motion capture system is a high-resolution, optical camera tracking system (OptiTrack, NaturalPoint, Corvallis, OR). The system contains 12 cameras, six camera stands, six camera mounts, multiple infrared reflective markers, a control box, and a computer interface and processing system (Motive Software, OptiTrack, NaturalPoint, Corvallis, OR). The cameras are strategically placed in the testing area to capture all views of the rigid body markers placed on the specimen.

The specimen is tracked by seven sets of 3D-printed, ABS-rigid body markers: five located at various positions

of interest on the arm, one on the rigid base plate, one on the humerus plate, and one on the front plate of the hand-rotation assembly. Calibrations of the cameras involve establishing a capture volume of the testing area, establishing a ground plane of the testing surface, and defining the rigid body marker sets for accurate tracking. Using motion capture technology in cadaveric testing helps create 3D modeling of motions with sub-millimeter accuracy. This subsequently allows for capturing the motions of multiple bodies in real time.

Validation Experiments

Overall, the main goal of the device is to deliver precise measurements of rotation, in a repeatable manner, without needing recalibration. To test the accuracy of the final design, calibrations were performed using three methods of angle measurement: a digital-angle gauge, the motion capture system, and the motor-control system (Figures 7A-7C and Figure 8). The digital-angle measurement was based on the tilt of the front 3D-printed nylon part of the hand-rotation assembly. The motion capture system gathered rotational information about the long axis of the specimen through the three retroreflective markers positioned on the front of the assembly. The motor-control system measured the angle of the hand-rotation assembly as defined by the user when positioning the joystick.

We used the specified rotation angle from the motor-control system as our baseline measurement. Output data from the three measures are shown in Table 1. We found a 2.2% error between the motor-control system and the digital-angle gauge and a 6.0% error between the motion capture system and the digital-angle gauge. Notably, this calibration was completed without a hand positioned in the device. When a hand was inserted, we noted increased resistance on the drive belt, which may cause a greater difference in error between the motor control system and the angle gauge. To accommodate this increase in torque resistance, it may be possible to increase the current to the NEMA 17 motor or upgrade to a NEMA 23 motor.

Table 1. Output data showing a comparison of the OptiTrack motion capture hand rotation assembly marker data, motor-control system, and digital-angle gauge.[a]

Position		OptiTrack	Motor Control	Digital Angle Gauge
Neutral		0	0	0
Pronation		19.28	20	20.3
		38.75	40	42.6
		59.25	60	60.7
Neutral		0	0	0.7
Supination		17.36	20	19.8
		37.26	40	39.6
		57.94	60	58.6
Neutral		0	0	0.4

[a] Motor control was used as the baseline data from which to compare the other two systems.

Figure 7. Various images of the forearm, showing positioning of the retroreflective markers on the 3D printed rigid bodies. (A) Distal radius and ulna. (B) Fixed humerus. (C) Proximal radius and ulna.

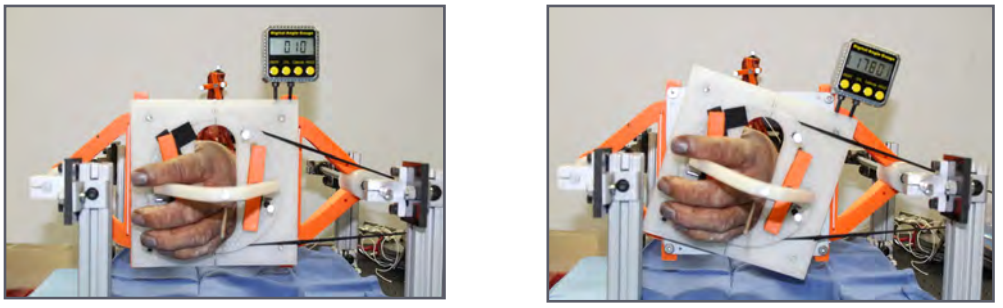

Figure 8. A digital angle gauge positioned on the top surface of the rotating face plate used for validation of the motion capture and motor control systems.

Active Pronation and Supination Option

In the passive configuration of this technology, the forearm rotated but only after rotations were applied to the hand. Owing to delays in carpometacarpal- and radiocarpal-load transmissions, there is a slight difference in angle between that of the hand and forearm. If the desired outcome is to examine these joints or interventions to these joints on upper-extremity motions, this device would be ideal in its current configuration. However, if the desire is to examine effects of intervention at the radio-humeral joint, distal or proximal radioulnar joint, or interosseous membrane, it may be preferable to apply active loads to the primary and secondary pronator and supinator tendons to produce pronation and supination motions of the forearm without lag effects caused by carpometacarpal or radiocarpal motions. With few modifications, the current technology can serve this purpose.

To change to an active control system, the baseplate, rail system, hand-rotation assembly, motion capture system, pulley system, and humerus plate would maintain their existing function. Only two modifications would be needed:

1) Isolation of the pronator teres, pronator quadratus (PQ), and supinator tendons (including the already isolated biceps brachii tendon) for active loading. Cable clamps can be attached to the tendons. Cables can be routed from the clamps through pulleys added to the baseplate, to apply direct loads to the tendons in the direction of their muscle pull. The secondary tendons (ie, PQ and supinator) can be loaded with constant weight corresponding to the desired load configuration method. For example, when pronation is desired, active tensile load can be applied to the pronator teres. A constant weight can be added to the PQ and supinator, with greater magnitude of weight on the PQ to simulate the force of muscle pull during pronation. The lighter weight on the supinator and biceps brachii simulates antagonistic muscle forces.

2) Remove the belt-drive system from around the hand-rotation assembly. This system could be placed proximal to the baseplate for applied loading. Alternatively, the system could be replaced with a linear-drive motor based on user preference. If the belt-drive system is maintained, the primary tendons (pronator teres and biceps brachii) could be coupled through their cable clamp systems. In this way, a desired rotation in pronation would result from an applied load to the pronator teres while the biceps brachii is unloaded. Similarly, a desired rotation in supination would result from an applied load to the biceps brachii while the pronator teres is unloaded. Figures 9A and 9B show an example of the active pronation and supination configuration possible with this technology.

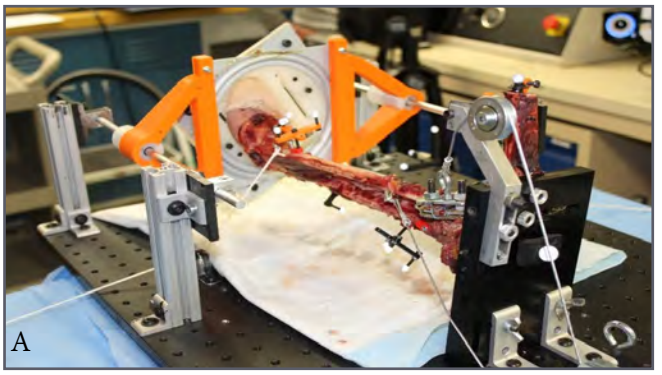

Figure 9. (A) Example of the device in active pronation/supination configuration. Yellow arrows show line of action of pull of the pronator teres and biceps brachii tendons during loading. (B) Placement of the linear motor system proximal to the baseplate to apply loads to the tendons while keeping the motor and associated electronic hardware clean from the cadaver testing.

Conclusion

When attempting to reproduce experimental results from other institutions, it is often difficult to achieve similar findings, partly because it is difficult to reproduce external testing methods. While technical details such as rate and direction of loading are often cited, most studies do not described details of their experimental setup.

This manuscript provides information on the development of a device to enable pronation and supination motions of a hand for use in cadaveric experimental studies. We provided a general overview of each component of the technology to enable an understanding of how each piece is essential to immobilizing the arm, controlling specific motions to simulate arm movement, and collecting the desired data outputs. This device may be used or adapted for use by institutions conducting similar research, so that the contributions to our field stem from an equivalent baseline of experimentation.

Funding

The authors received no financial support for the research, authorship, and publication of this article.

Conflict of Interest

The authors report no conflicts of interest.